

Measurement of the c -Axis Optical Reflectance of $A\text{Fe}_2\text{As}_2$ ($A = \text{Ba}, \text{Sr}$) Single Crystals: Evidence of Different Mechanisms for the Formation of Two Energy Gaps

Z. G. Chen, T. Dong, R. H. Ruan, B. F. Hu, B. Cheng, W. Z. Hu, P. Zheng, Z. Fang, X. Dai, and N. L. Wang

Beijing National Laboratory for Condensed Matter Physics, Institute of Physics, Chinese Academy of Sciences, Beijing 100190, China

(Received 12 January 2010; revised manuscript received 21 June 2010; published 27 August 2010)

We present the c -axis optical reflectance measurement on single crystals of BaFe_2As_2 and SrFe_2As_2 , the parent compounds of FeAs based superconductors. Different from the ab -plane optical response where two distinct energy gaps were observed in the spin-density-wave (SDW) state, only the smaller energy gap could be seen clearly for $\mathbf{E} \parallel c$ axis. The very pronounced energy gap structure seen at a higher energy scale for $\mathbf{E} \parallel ab$ plane is almost invisible. We propose a novel picture for the band structure evolution across the SDW transition and suggest different driving mechanisms for the formation of the two energy gaps.

DOI: 10.1103/PhysRevLett.105.097003

PACS numbers: 74.25.Gz, 74.70.Xa, 75.30.Fv

For quasi-two-dimensional layered materials, striking differences could exist in the in-plane and out-of-plane charge transport and dynamics. For example, in some high- T_c cuprates, metallic in-plane charge transport coexists with nonmetallic conductivity along the c axis [1,2]. The contrasting behavior violates the conventional concept of band electron transport, and has been the subject of intensive study. Fe-pnictide superconducting materials also crystalize in the layered structure with FeAs layers separated by alkaline metal ions or other insulatorlike layers. Band structure calculations based on the local-density approximation (LDA) or generalized gradient approximations (GGA) indicate dominantly two-dimensional (2D) cylinderlike Fermi surfaces (FSs) along the c axis [3–5]. It is important to see whether or not the Fe pnictides share similar anisotropic charge dynamical properties with cuprates.

Optical spectroscopy is a powerful technique to investigate charge dynamics and band structure of a material as it probes both free carriers and interband excitations. In particular, it yields direct information about the energy gap formation in the broken symmetry state. Optical spectroscopy studies on the ab -plane properties of different Fe-pnictides and chalcogenides systems have been reported by several groups [6–18]. For the parent compounds of Fe pnictides, the measurements provide clear evidence for the formation of the partial energy gaps in the magnetic phase, supporting the itinerant picture that the energy gain for the antiferromagnetic ground state is achieved through the opening of a spin-density-wave (SDW) gap on the FSs [7,10,14–16]. For the superconducting samples, the superconducting pairing gaps were also detected by the technique [6,17,18]. However, optical investigations have not been carefully done on the c -axis response of Fe-pnictide materials. There is only one work in the literature containing optical data along the c axis [10]. Unfortunately, the data were limited to the high frequencies, above 700 cm^{-1} . Because of this limitation, neither the free-carrier response

nor any feature related to the SDW gap were observed. In fact, the reported reflectance data appear to have extraordinarily low values. As information about the anisotropic charge dynamics is extremely important for understanding the materials, a detailed and careful determination of the c -axis optical response is highly necessary.

In this Letter we present the c -axis ($\mathbf{E} \parallel \mathbf{c}$) optical reflectance measurement over broad frequencies on thick BaFe_2As_2 and SrFe_2As_2 single crystal samples. We observed the SDW energy gap formation in the low- T magnetic ordered state. However, different from the ab -plane response where two distinct energy gaps were identified for $A\text{Fe}_2\text{As}_2$ ($A = \text{Ba}, \text{Sr}$), only the gap corresponding to the smaller energy scale of $\mathbf{E} \parallel ab$ plane could be clearly seen for the polarization parallel to the c axis. The more pronounced gap structure at the higher energy scale for $\mathbf{E} \parallel ab$ plane becomes almost invisible. The significant difference between the two polarizations has an important implication for the electronic structure of those compounds. A schematic picture for the band structure evolution across the structural or magnetic transition was proposed to understand the experimental findings.

Large-sized single crystals of BaFe_2As_2 and SrFe_2As_2 were grown from the FeAs flux in Al_2O_3 crucibles sealed in quartz tubes. The growth procedure is similar to the description in our earlier work [19] except for one major difference: the crucible and quartz tube were placed in a direction of 45° relative to the vertical. After completing the growth procedure and breaking the crucible, we can easily find relatively thick crystals growing from the inner surface of the crucible along the direction at 45° relative to the crucible cylinder axis (i.e., crystals grow vertically). The dc resistivity measured by the four contact techniques on the cleaved ab plane was found to be almost identical to the data presented in our early work, showing sharp drops at 138 K and 200 K for BaFe_2As_2 and SrFe_2As_2 , respectively, being ascribed to the formation of SDW order [7]. We performed x-ray diffraction measurement to check the

single crystalline nature of our samples and their orientation. The crystals were then cut in a direction perpendicular to the cleaved ab plane. The cutting surfaces were finely polished for the c -axis polarization measurement.

The optical reflectance measurements with $\mathbf{E} \parallel c$ axis were performed on a Bruker IFS 66v/s spectrometer in the frequency range from 50 to 25 000 cm^{-1} . An *in situ* gold and aluminum overcoating technique was used to get the reflectivity $R(\omega)$. The real part of conductivity $\sigma_1(\omega)$ is obtained by the Kramers-Kronig transformation of $R(\omega)$. A Hagen-Rubens relation was used for low frequency extrapolation. A $\omega^{-0.5}$ dependence was used for high frequency extrapolation up to 300 000 cm^{-1} , above which a ω^{-4} dependence is employed.

Figure 1 shows the c -axis $R(\omega)$ and $\sigma_1(\omega)$ at room temperature over a broad frequency range up to 20 000 cm^{-1} for BaFe_2As_2 . For a comparison, we also plot the optical spectra with the $\mathbf{E} \parallel ab$ plane [7]. We can see that the overall $R(\omega)$ along the c axis is quite similar to that in the ab plane except for relatively lower values. This is dramatically different from the optical spectra of some high- T_c cuprates [2] and other layered compounds, for example, layered ruthenates [20], where the c axis $R(\omega)$ shows much lower values and quite different frequency-dependent behavior from the ab plane. This observation suggests that the band structure of Fe pnictide should be quite three-dimensional (3D), in contrast to the expectation based on its layered crystal structure. The difference in $\sigma_1(\omega)$ spectra between ab plane and the c axis seems to become larger at low frequencies. An extrapolation to zero frequency, or the dc conductivity, shows an anisotropy ratio of about 2.8. This matches well with the anisotropy ratio determined directly from the dc resistivity measurement by a careful Montgomery technique (about 3 ± 1) [21]. We noticed that the c -axis reflectance values obtained here are much higher than the data presented by Wu *et al.* on a EuFe_2As_2 sample [10]. The reflectance

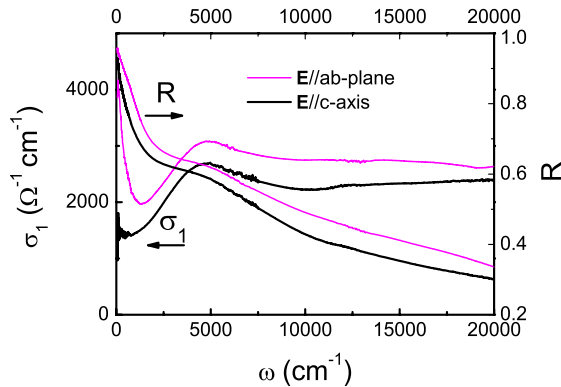


FIG. 1 (color online). The c axis $R(\omega)$ and $\sigma_1(\omega)$ at 300 K for BaFe_2As_2 over broad frequencies up to 20 000 cm^{-1} . The ab -plane spectra were also included for the purpose of comparison [7]. The conductivity anisotropy at low frequency limit is about 2.8.

values in their measured frequency range (above 700 cm^{-1}) are already below 0.4, leading to extremely low values of conductivity (below $100 \Omega^{-1} \text{cm}^{-1}$ at 700 cm^{-1}). We remark here that we repeated measurement of $\mathbf{E} \parallel c$ on another crystal grown from a different batch and achieved almost identical results.

The temperature dependences of the $R(\omega)$ and $\sigma_1(\omega)$ spectra of BaFe_2As_2 below 7000 cm^{-1} (~ 1 eV) are plotted in Figs. 2(a) and 2(b), respectively. In the midinfrared region (near 4000 cm^{-1}), there is a strong suppression feature in both $R(\omega)$ and $\sigma_1(\omega)$ spectra. Essentially, the same feature is seen in the ab -plane optical response at slightly higher frequencies (near 5000 cm^{-1}). For a comparison we also plot the in-plane $R(\omega)$ and $\sigma_1(\omega)$ spectra at 300 K and 10 K in the figure [7]. The suppressed spectral weight in $\sigma_1(\omega)$ is largely transferred to the high frequencies above 5000 cm^{-1} for both polarizations. The suppression is a common feature for Fe-pnictide materials and is not directly related to the SDW order as it is seen well above the structural or magnetic transition temperature [7,13,16]. Its origin remains to be explored. Most remarkably, the reflectance is strongly suppressed below $\sim 320 \text{ cm}^{-1}$ upon entering the SDW ordered state. A sharp upturn appears at lower energy scale. The strong suppression in $R(\omega)$ results in a prominent gap structure in $\sigma_1(\omega)$. The sharp upturn at lower frequencies in $R(\omega)$ leads to a narrow residual Drude component at very low frequencies

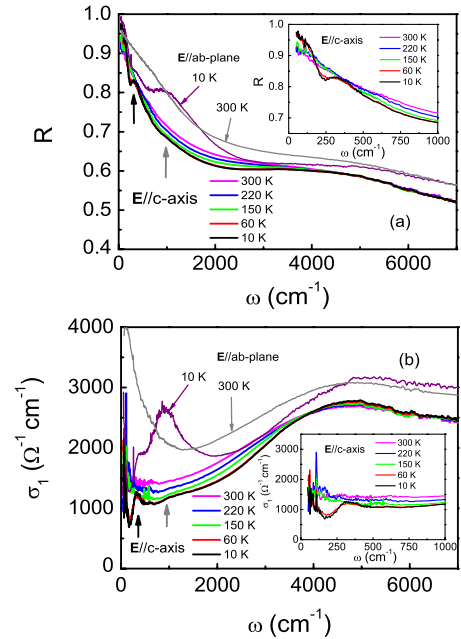


FIG. 2 (color online). The c axis $R(\omega)$ (a) and $\sigma_1(\omega)$ (b) at different temperatures below 7000 cm^{-1} for BaFe_2As_2 . Inset: expanded plot of the low- ω $R(\omega)$ and $\sigma_1(\omega)$ spectra. The ab -plane $R(\omega)$ and $\sigma_1(\omega)$ at 300 K and 10 K are included for comparison. The two upward arrows indicate the anomalies associated with the SDW order. The very pronounced peak in $\sigma_1(\omega)$ for $\mathbf{E} \parallel ab$ plane becomes extremely weak for $\mathbf{E} \parallel c$.

[see the insets of Figs. 2(a) and 2(b)]. Above T_{SDW} , the Drude feature is not clear for $\mathbf{E} \parallel c$ axis, being different from the spectra in the ab plane. The data provide clear evidence for the partial energy gap formation along the c axis in the SDW ordered phase as well. In the ab -plane optical spectra [7], we observed two energy gaps in the SDW state with the conductivity peak energies near 360 cm^{-1} and 890 cm^{-1} . Here we found that the energy scale of the gap for $\mathbf{E} \parallel c$ is close to the smaller one seen in the ab plane $\sigma_1(\omega)$. The more pronounced gap structure at higher energy in the ab plane becomes extremely weak for the c -axis polarization in both $R(\omega)$ and $\sigma_1(\omega)$, as indicated by an upward grey arrow in the figure.

It is tempting to analyze the data in a more quantitative way. Since a residual narrow Drude component is present at very low temperature in the SDW state, it is relatively easy to isolate its spectral weight. We use a standard Drude-Lorentz model to decompose the spectra into different components:

$$\epsilon(\omega) = \epsilon_\infty - \frac{\omega_p^2}{\omega^2 + i\omega/\tau} + \sum_{i=1}^N \frac{S_i^2}{\omega_i^2 - \omega^2 - i\omega/\tau_i}. \quad (1)$$

Here, ϵ_∞ is the dielectric constant at high energy, the middle and last terms are the Drude and Lorentz components, respectively. The experimental $R(\omega)$ and $\sigma_1(\omega)$ spectra at 10 K could be well reproduced by using a Drude and several Lorentz peaks, as shown in Fig. 3 [22]. This analysis leads to $\omega_{pc} = 3600 \text{ cm}^{-1}$ and $1/\tau_c = 47 \text{ cm}^{-1}$ for the Drude component at 10 K. Our earlier study on the ab -plane properties indicates that those two parameters are 4660 cm^{-1} and 55 cm^{-1} at 10 K, respectively [7]. Then we find that the anisotropy ratio of the spectral weight, which is equal to the ratio of the square of plasma frequency $\omega_{pc}^2/\omega_{pab}^2$, is about 60% at 10 K. The value indicates that the anisotropy of the band structure

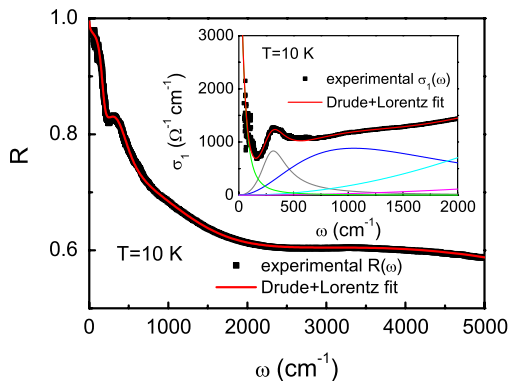


FIG. 3 (color online). The experimental $R(\omega)$ (main panel) and $\sigma_1(\omega)$ (inset) at 10 K of BaFe_2As_2 for $\mathbf{E} \parallel c$ and the fitting curves from a Drude-Lorentz model up to different energy scales at 10 K. The same parameters were used to reproduce both $R(\omega)$ and $\sigma_1(\omega)$. The decomposed Drude component and the Lorentz peaks are also shown in the inset.

reconstructed in the SDW order state is not very strong. Since the Drude-like features above T_{SDW} are not very clear, there is no unique or unambiguous way to isolate the Drude components from the overall spectra, we did not try to estimate those parameters at high temperatures.

The substantial difference of low frequency gap structures in the SDW state between the two polarizations has important implication for the electronic structure of Fe pnictides. It is important to check whether the observations are generic for 122-type parent compounds. For this purpose, we performed optical measurement on SrFe_2As_2 single crystals. Because the obtained SrFe_2As_2 crystals have smaller dimension along the c axis, the signal-to-noise ratio at low frequencies is much smaller. Nevertheless, we observed essentially the same spectral features for SrFe_2As_2 as well. As shown in Fig. 4, only the smaller gap could be seen for $\mathbf{E} \parallel c$ axis in the SDW state, the large energy gap is almost invisible. Those experiments indicate that the observed spectral features are generic for 122-type undoped compounds.

Understanding why two distinct gaps could be observed for $\mathbf{E} \parallel ab$ plane but only a smaller one could be clearly seen for $\mathbf{E} \parallel c$ axis is a crucial issue here. It has an important implication for the band structure evolution across the transition. We found that our data could be naturally explained by assuming that there are two types of FSs in the system: the 2D cylinderlike FSs and a large-size 3D ellipsoid like FS, as schematically presented in Fig. 5. Presence of the large-size 3D ellipsoid FS with

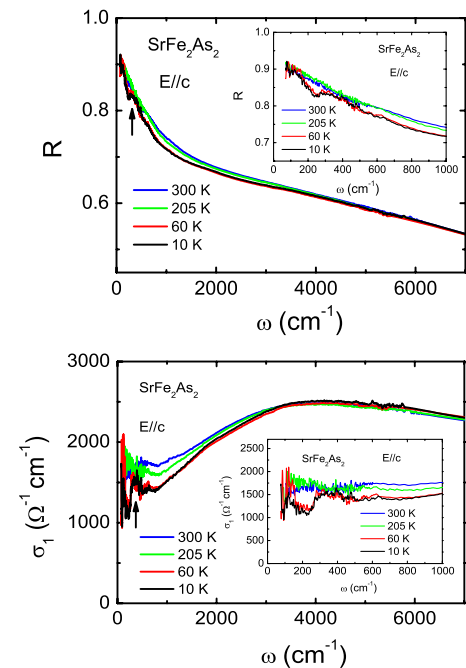


FIG. 4 (color online). The c -axis $R(\omega)$ and $\sigma_1(\omega)$ at different temperatures below 7000 cm^{-1} for SrFe_2As_2 . Inset: expanded plot of the low- ω $R(\omega)$ and $\sigma_1(\omega)$ spectra. The upward arrows indicate the anomalies associated with the SDW order.

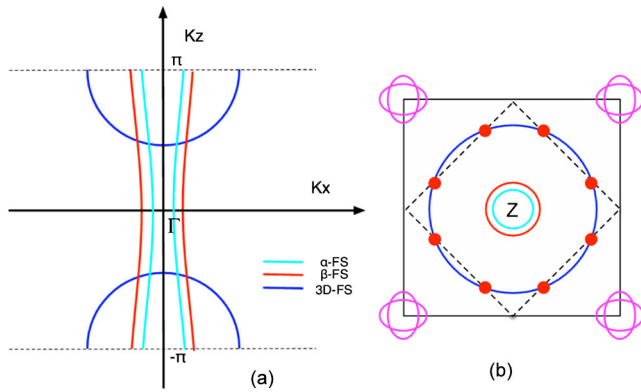


FIG. 5 (color online). (a) The schematic plot of the Fermi surfaces along the k_z direction around the Γ point. Besides the 2D FSs (α and β bands) there is an additional 3D FS enclosing the Z point $[(0, 0, \pi)]$. (b) A top view of the FSs. The magnetic Brillouin zone driven by the (π, π) nesting between the disconnected 2D cylinderlike FSs would cut the 3D FS and open gaps in the intersecting points.

dominant $\text{Fe-}3d_{3z^2-r^2}$ orbital is indicated by the recent *ab initio* LDA + Gutzwiller calculations, where electron correlations are taken into account beyond LDA [23]. Recent transport [21], upper critical field [24], as well as ARPES experiments [25,26] also suggest the presence of a 3D FS.

If we neglect the small dispersion of those 2D FSs along the c axis, the Fermi velocity along the c axis becomes zero and the electrons on the 2D FSs would only couple to the polarized light with $\mathbf{E} \parallel ab$ plane. On the other hand, the electrons on the 3D FS can couple to the light polarized along any direction. We suggest that the 2D cylinderlike hole FSs around Γ and the 2D electron FSs around the corner of the Brillouin zone are strongly nested, which is the main driving force for the SDW instability of the system, while the 3D ellipsoid FS does not show any nesting with other FSs. Nevertheless, with the formation of the SDW order driven by the (π, π) nesting of 2D FSs, the new magnetic Brillouin zone boundary would cut the large-size 3D ellipsoid FS and result in an energy gap at the intersecting points as shown in Fig. 5(b). This can be seen by optics in both $\mathbf{E} \parallel ab$ plane and $\mathbf{E} \parallel c$. Then we ascribe the larger gap seen most clearly for $\mathbf{E} \parallel ab$ plane to the nesting-driven gap opened on 2D FSs, the smaller one to the gap formed on the 3D FS which could be considered as the consequence of the SDW order. Because the 2D FSs are more dramatically affected by the SDW instability than the 3D FS, we expect a reduction of the anisotropy in the magnetic ordered state.

To summarize, we have successfully grown thick single crystals of AFe_2As_2 ($A = \text{Ba, Sr}$) and investigated their optical properties. Our study revealed a clear difference in

optical conductivity for $\mathbf{E} \parallel ab$ plane and $\mathbf{E} \parallel c$ axis in the SDW state. The very pronounced energy gap structure seen at a higher energy scale for $\mathbf{E} \parallel ab$ plane is almost invisible for $\mathbf{E} \parallel c$ axis, whereas the smaller energy gap could be seen in both polarizations. We propose a novel picture for the band structure evolution and suggest different driving mechanisms for the two energy gaps. The strong (π, π) nesting between disconnected 2D cylinderlike FSs is the main driving force for the SDW instability, leading to the opening of larger energy gaps in the 2D FSs. The cutting of the magnetic Brillouin zone on the 3D FS leads to a smaller gap at the crossing region.

This work is supported by the National Science Foundation of China, the Knowledge Innovation Project of the Chinese Academy of Sciences, and the 973 project of the Ministry of Science and Technology of China.

-
- [1] Y. Ando *et al.*, *Phys. Rev. Lett.* **77**, 2065 (1996).
 - [2] S. Uchida, K. Tamasaku, and S. Tajima, *Phys. Rev. B* **53**, 14 558 (1996).
 - [3] S. Lebegue, *Phys. Rev. B* **75**, 035110 (2007).
 - [4] D. J. Singh and M. H. Du, *Phys. Rev. Lett.* **100**, 237003 (2008).
 - [5] Fengjie Ma and Zhong-Yi Lu, *Phys. Rev. B* **78**, 033111 (2008).
 - [6] G. Li *et al.*, *Phys. Rev. Lett.* **101**, 107004 (2008).
 - [7] W. Z. Hu *et al.*, *Phys. Rev. Lett.* **101**, 257005 (2008).
 - [8] F. Pfuner *et al.*, *Eur. Phys. J. B* **67**, 513 (2009).
 - [9] J. Yang *et al.*, *Phys. Rev. Lett.* **102**, 187003 (2009).
 - [10] D. Wu *et al.*, *Phys. Rev. B* **79**, 155103 (2009).
 - [11] M. M. Qazilbash *et al.*, *Nature Phys.* **5**, 647 (2009).
 - [12] G. F. Chen *et al.*, *Phys. Rev. B* **79**, 140509(R) (2009).
 - [13] W. Z. Hu *et al.*, *Phys. Rev. B* **80**, 100507(R) (2009).
 - [14] A. Akrap *et al.*, *Phys. Rev. B* **80**, 180502(R) (2009).
 - [15] S. J. Moon *et al.*, *Phys. Rev. B* **81**, 205114 (2010).
 - [16] Z. G. Chen *et al.*, *Phys. Rev. B* **81**, 100502(R) (2010).
 - [17] E. van Heumen *et al.*, *Europhys. Lett.* **90**, 37005 (2010).
 - [18] K. W. Kim *et al.*, *Phys. Rev. B* **81**, 214508 (2010).
 - [19] G. F. Chen *et al.*, *Phys. Rev. B* **78**, 224512 (2008).
 - [20] T. Katsufuji, M. Kasai, and Y. Tokura, *Phys. Rev. Lett.* **76**, 126 (1996).
 - [21] M. A. Tanatar *et al.*, *Phys. Rev. B* **79**, 134528 (2009).
 - [22] The low- and midinfrared $R(\omega)$ and $\sigma_1(\omega)$ could be well reproduced by one Drude and three Lorentz components centered at 320, 1000, and 4500 cm^{-1} (for SDW gap and interband transitions). To reproduce the spectra up to 20 000 cm^{-1} , one extra Lorentz term at higher energy has to be added.
 - [23] G. T. Wang *et al.*, *Phys. Rev. Lett.* **104**, 047002 (2010).
 - [24] H. Q. Yuan *et al.*, *Nature (London)* **457**, 565 (2009).
 - [25] C. Liu *et al.*, *Phys. Rev. Lett.* **101**, 177005 (2008).
 - [26] W. Malaeb *et al.*, *J. Phys. Soc. Jpn.* **78**, 123706 (2009).